Journal of Physics: Condensed Matter

From underdoped to overdoped cuprates: two quantum phase transitions

J. Phys.: Condens. Matter **23** (2011) 045701 (6pp) doi:10.1088/0953-8984/23/4/045701

From underdoped to overdoped cuprates: two quantum phase transitions

S G Ovchinnikov[1,2], E I Shneyder[1,3] and M M Korshunov[1,4]

[1] L V Kirensky Institute of Physics, Siberian Branch of Russian Academy of Sciences, 660036 Krasnoyarsk, Russia
[2] Siberian Federal University, Krasnoyarsk 660041, Russia
[3] Reshetnev Siberian State Aerospace University, Krasnoyarsk 660014, Russia
[4] Department of Physics, University of Florida, Gainesville, FL 32611, USA

E-mail: korshunov@phys.ufl.edu

Received 15 September 2010, in final form 14 December 2010
Published 12 January 2011
Online at stacks.iop.org/JPhysCM/23/045701

Abstract

Several experimental and theoretical studies indicate the existence of a critical point separating the underdoped and overdoped regions of the high-T_c cuprates' phase diagram. There are at least two distinct proposals on the critical concentration and its physical origin. The first one is associated with the pseudogap formation for $p < p^*$, with $p^* \approx 0.2$. The other relies on the Hall effect measurements and suggests that the critical point and the quantum phase transition (QPT) take place at optimal doping, $p_{opt} \approx 0.16$. Here we have performed a precise density of states calculation and found that there are two QPTs and the corresponding critical concentrations associated with the change of the Fermi surface topology upon doping.

(Some figures in this article are in colour only in the electronic version)

1. Introduction

The mystery of high-T_c superconductivity in layered cuprates is closely related to their common pattern of doping dependent transitions from an antiferromagnetic insulator at zero doping to an overdoped metal. A number of experimental and theoretical studies have indicated that the transition is not smooth and a critical point separates the underdoped (UD) and overdoped (OD) regions. It is tempting to associate such a critical point with the pseudogap formation for $p < p^*$, with $p^* = 0.19$–0.24 [1–5]. There is no doubt that the proximity of the pseudogap and the superconductivity with two energy scales, T^* and T_c, is essential for high-T_c superconductivity [6]. On the other hand, the Hall effect measurements suggest that the critical point and the quantum phase transition (QPT) take place at optimal doping, $p_{opt} = 0.16$ [7, 8]. To resolve this controversy, here we study the doping dependent electronic structure of the single-layer cuprate like $La_{2-x}Sr_xCuO_4$ in the regime of strong electron correlation within the t–t'–t''–J^* model. By a very precise density of states (DOS) calculation we have found two QPTs associated with the changes of the Fermi surface (FS) topology. At optimal doping, $x_{c1} = p_{opt} = 0.151$, the DOS reveals the logarithmic divergence while at the pseudogap QPT, $x_{c2} = p^* = 0.246$, there is a Heaviside-type step in the DOS.

Angle-resolved photo-emission spectroscopy (ARPES) reveals a change of the FS topology from the small hole pockets to the large hole FS near the optimal doping [9, 10]. This provides a link between the QPT and changes of the FS. Here we apply the general Lifshitz ideas [11] on the QPT induced by the FS transformations, but first we will discuss how these transformations are induced by doping.

It is easy to obtain a large FS in cuprates by a single-electron approach such as the local density approximation (LDA) or the tight-binding method. However, to get the small hole pockets around the $(\pm\pi/2, \pm\pi/2)$ points of the Brillouin zone one has to go beyond the weak-coupling approximations and take the strong electronic correlations into account. Such small pockets have been found in a doped antiferromagnetic (AFM) Mott insulator by exact diagonalization [12, 13] and quantum Monte Carlo calculations [14, 15] for the finite clusters as well as by a perturbative treatment of the infinite lattice [16–19] and by using the slave-particles [20, 21]. According to these studies, after the long-range AFM order vanishes with increasing hole concentration $n_h = 1 + p$ (in $La_{2-x}Sr_xCuO_4$, $p = x$), a short-range AFM order still persists even at optimal doping [22]. The short-range magnetic order determines the self-energy and hole dispersion resulting in the small hole pockets around the $(\pm\pi/2, \pm\pi/2)$ points

in the UD cuprates; its fluctuation results in the pseudogap formation [23–25]. Due to the strong electronic correlations intrinsic for cuprates, a theory of the electron dynamics has to fulfil a 'no-double occupancy' constraint. This constraint is introduced explicitly in the mean-field theory of a d-type superconductivity within the RVB approach [26] for the t–J model [27], and in the variational Monte Carlo studies [28].

2. Method

Contrary to the phenomenological approaches, such as assuming that the second order QPT exists at $p = p_c$ [29], we deal with a microscopically derived t–t'–t''–J^* model without free parameters. To properly fulfil the 'no-double occupancy' constraint at every step of our calculations we use the Hubbard X-operators, $X^{hg} = |h\rangle\langle g|$, where $|h\rangle$ and $|g\rangle$ are the local eigenvectors corresponding to three states: one-hole states $|\sigma\rangle$, $\sigma = \pm 1/2$, and the Zhang–Rice singlet, $|S\rangle$, which is a two-hole state. The relation between X-operators and single-electron annihilation operators is given by $a_{f\sigma} = \sum_{h,g} \gamma_\sigma(h,g) X_f^{hg}$, where the coefficients $\gamma_\sigma(h,g)$ determine the partial weight of the quasiparticle excitation $g \to h$ in the process of a particle annihilation on site f with spin σ. The 'no-double occupancy' constraint means the absence of direct excitations from and to the lower Hubbard band and the exclusion of the two-electron (zero-hole) state $|0\rangle = \mathrm{d}^{10}\mathrm{p}^6$ from the local Hilbert space. It is demonstrated straightforwardly by the exact calculation of the two-electron state occupation number that $\langle n_{f\uparrow} n_{f\downarrow}\rangle = \langle X_f^{00}\rangle = 0$; this constraint is provided by X-operator algebra. Nevertheless the virtual interband (between the lower and upper Hubbard bands) hopping t_{fg}^{12} results in the exchange interaction $J_{fg} = (t_{fg}^{12})^2/U_{\mathrm{eff}}$.

For $La_{2-x}Sr_xCuO_4$, all intraband and interband hopping parameters (t_{fg}^{11} and t_{fg}^{12}), single-site energies of holes in p- and d-orbitals, and the charge transfer gap U_{eff} have been calculated by the *ab initio* LDA + GTB approach [30] which combines LDA and the generalized tight-binding (GTB) method for strongly correlated systems. The low energy effective model is the t–t'–t''–J^* model where J^* means that besides the Heisenberg exchange term a three-site correlated hopping H_3 is also included, $H_{t-J^*} = H_{tJ} + H_3$, where

$$H_{tJ} = \sum_{f,\sigma}(\varepsilon-\mu)X_f^{\sigma\sigma} + \sum_f 2(\varepsilon-\mu)X_f^{SS} + \sum_{f\neq g,\sigma}\left[t_{fg}^{11}X_f^{S\bar\sigma}X_g^{\bar\sigma S} + \frac{J_{fg}}{4}(X_f^{\sigma\bar\sigma}X_g^{\bar\sigma\sigma} - X_f^{\sigma\sigma}X_g^{\bar\sigma\bar\sigma})\right],$$

$$H_3 = \sum_{f\neq m\neq g,\sigma}\frac{t_{fm}^{12}t_{mg}^{12}}{U_{\mathrm{eff}}}\left(X_f^{\sigma S}X_m^{\bar\sigma\sigma}X_g^{S\bar\sigma} - X_f^{\sigma S}X_m^{\bar\sigma\bar\sigma}X_g^{S\sigma}\right).$$

Here the hole creation operator is now $\tilde a_{f\sigma}^\dagger = 2\sigma X_f^{S\bar\sigma}$ and its algebra is different from the bare fermion's one ($2\sigma = \pm 1$ for $\sigma = \uparrow, \downarrow$). The spin operators are also easily expressed via X-operators, $S_f^+ = X_f^{\sigma\bar\sigma}$, $S_f^z = (X_f^{\sigma\sigma} - X_f^{\bar\sigma\bar\sigma})/2$.

Our approach is essentially a perturbation theory with the small parameter t/U contrary to the usual Fermi liquid perturbation expansion in terms of U which is large in cuprates. We use a method of irreducible Green's functions which is similar to the Mori-type projection technique, with the zero-order Green's function given by the well-known Hubbard I approximation. Beyond it there are spin fluctuations. To provide a description of them, the self-energy was calculated in the non-crossing approximation by neglecting vertex renormalization that is equivalent to the self-consistent Born approximation (SCBA) [31]. The resulting electron self-energy contains the space–time dependent spin correlation function $C(\mathbf{q},\omega)$ and results in the finite quasiparticle lifetime, $\mathrm{Im}\,\Sigma(\mathbf{k},\omega) \neq 0$. Note that at low temperatures $T \leqslant 10$ K the spin dynamics is much slower than the electron one. A typical spin fluctuation time, 10^{-9} s, is much larger than the electronic time 10^{-13} s [32]; that is why we can safely neglect the time dependence of the spin correlation function, $C(\mathbf{q},\omega) \to C_{\mathbf{q}}$. The self-energy becomes static, $\Sigma(\mathbf{k},\omega) \to \Sigma(\mathbf{k})$, and we have $\mathrm{Im}\,\Sigma = 0$. Note that $\Sigma(\mathbf{k},\omega)$ here is the object, which is completely different from the one in the Fermi liquid approach because here it is built by the diagrams for the X-operators, not the standard Fermionic annihilation–creation operators $a_{f\sigma}$. In the usual Fermi liquid expansion, dynamical self-energy definitely plays a crucial role in the lightly doped cuprates. Here, our theory starts from a different limit where the lowest order approximation is represented by the Hubbard I solution. The corrections to the strongly correlated mean-field approach are small because the starting point is already a reasonable approximation for the Mott–Hubbard insulator. That is proved by the small effect of the frequency dependence of the self-energy in [34, 31]. Moreover, the doping dependence of the FS is determined by $\mathrm{Re}\,\Sigma$, and it is qualitatively similar in our approach [33] and in the approach which properly takes $\mathrm{Im}\,\Sigma$ into account [34, 31].

The vertex corrections to the self-energy are small far from the spin–density wave or the charge-density wave instabilities, which is true for moderate doping. Our approximation for the self-energy is done in the framework of the mode-coupling approximation which has been proved to be quite reliable even for systems with strong interaction [35, 36]. As shown in the spin-polaron treatment of the t–J model, the vertex corrections to the non-crossing approximation are small and give only numerical renormalization of the model parameters [37].

The Green's function $\langle\langle X_{\mathbf{k}}^{\bar\sigma S}|X_{\mathbf{k}}^{S\bar\sigma}\rangle\rangle_\omega$ for a hole moving on the background of short-range AFM order is

$$G(\mathbf{k},\omega) = \frac{(1+x)/2}{\omega - \varepsilon + \mu - \frac{1+x}{2}t_{\mathbf{k}} - \frac{1-x^2}{4}\frac{\tilde t_{\mathbf{k}}^2}{U_{\mathrm{eff}}} + \Sigma(\mathbf{k})}, \qquad (1)$$

where

$$\Sigma(\mathbf{k}) = -\frac{2}{1+x}\frac{1}{N}\sum_{\mathbf{q}}\left\{\left[t_{\mathbf{k}-\mathbf{q}} - \frac{1-x}{2}J_{\mathbf{q}} + \frac{1-x}{2}\frac{\tilde t_{\mathbf{k}-\mathbf{q}}^2}{U_{\mathrm{eff}}} - \frac{1+x}{2}\frac{2\tilde t_{\mathbf{k}}\tilde t_{\mathbf{k}-\mathbf{q}}}{U_{\mathrm{eff}}}\right]\left(\frac{3}{2}C_{\mathbf{q}} + K_{\mathbf{k}-\mathbf{q}}\right) - \frac{1+x}{2}\frac{\tilde t_{\mathbf{q}}^2}{U_{\mathrm{eff}}}K_{\mathbf{q}}\right\}.$$

Here, $t_{\mathbf{k}}$ and $\tilde t_{\mathbf{k}}$ are the Fourier transforms of hoppings t_{fg}^{11} and t_{fg}^{12}, respectively. The self-energy is determined by static spin correlation function $C_{0n} = \langle S_0^+ S_n^-\rangle$ and kinetic correlation function $K_{0n} = \sum_\sigma \langle \tilde a_{0\sigma}^\dagger \tilde a_{n\sigma}\rangle$ between sites 0 and n. These correlation functions and their Fourier transforms $C_{\mathbf{q}}$

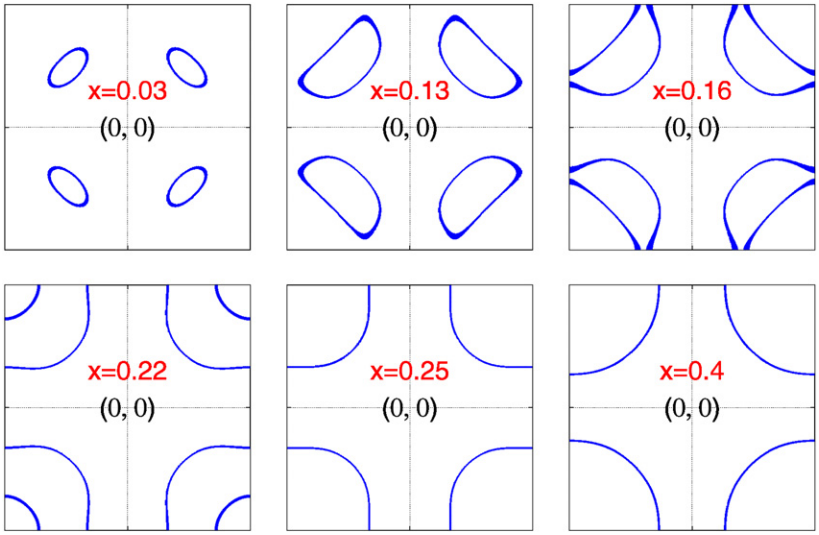

Figure 1. Mean-field FS transitions with doping x as calculated from poles of equation (1). There are two topological changes: the first one between $x = 0.13$ and 0.16, and the second one between 0.22 and 0.25; see [33] for detailed discussion.

and $K_{\mathbf{q}}$ represent the AFM short-range order and the valence-bond order, respectively. In contrast to the approach of [31], we calculate these correlation functions self-consistently up to $n = 9$ (ninth coordination sphere) together with the chemical potential μ. To get the spin correlation function we also obtain the spin Green's function $\langle\langle X^{\sigma\bar{\sigma}}_{\mathbf{q}} | X^{\bar{\sigma}\sigma}_{\mathbf{q}} \rangle\rangle_\omega$ in a spherically symmetric spin liquid state [38, 39] with $\langle S^z \rangle = 0$ and the equal correlation functions for each spin component, $\langle S^+_0 S^-_n \rangle = 2\langle S^z_0 S^z_n \rangle = C_{0n}$. Both C_{0n} and K_{0n} are essentially doping dependent and C_{0n} decrease with the doping [33]. While the nearest neighbor function C_{01} is finite for all studied x up to $x = 0.4$ with a kink at $x = p^* = 0.24$, more distant spin correlations fall down to zero for $x > p^*$.

The calculated FS twice changes its topology with doping [33], see figure 1. Small hole pockets around $(\pm\pi/2, \pm\pi/2)$ points are present at small doping; then they increase in size and touch each other in the non-symmetric points $\mathbf{k} = \pm\pi(1, \pm 0.4)$ at $x_{c1} = p_{opt} = 0.151$. Above p_{opt}, there are two FSs around (π, π) with the outer one being hole-like and inner being electron-like. The electron FS collapsed at $x_{c2} = p^* = 0.246$, and at $x > p^*$ we have only one large hole surface around (π, π). A similar conclusion on the coexistence of hole and electron FSs at some intermediate doping have been also drawn recently [40, 41], and earlier for the spin–density wave state of the Hubbard model [42].

It should be stressed that the standard DOS calculations with routine precision (400×400 points in the quarter of the Brillouin zone) which we used before to solve the T_c equation for the magnetic mechanism of $d_{x^2-y^2}$-wave pairing [46] is not enough to find the effect of QPT on DOS. To get the results presented below we used $10^4 \times 10^4$ k-points which lead to an increase of precision by 625 times.

3. Results

From the previous consideration it follows that the FS topological transitions in cuprates are induced by doping and they are due to the non-rigid band behavior of the quasiparticles in the strongly correlated systems. According to the general Lifshitz analysis [11] for the three-dimensional (3D) system, a change of topology at the energy $\varepsilon = \varepsilon_c$ either by the appearance of a new segment (such as we found at p^*) or by change of its connectivity (such as at p_{opt}) would result in the additional DOS, $\delta N(\varepsilon) \sim (\varepsilon - \varepsilon_c)^{1/2}$, and a change in the thermodynamic potential, $\delta\Omega \sim (\varepsilon_F - \varepsilon_c)^{5/2}$ (the QPT is of order 2.5), where ε_F is the Fermi energy. However, due to the strong anisotropy of electronic and magnetic properties, cuprates are quasi-two-dimensional (2D) and not isotropic 3D systems. The electron hopping perpendicular to the CuO_2 layers in a single-layer $La_{2-x}Sr_xCuO_4$ (LSCO), $Bi_2Sr_2CuO_{6+\delta}$ (Bi2201), etc is negligibly small. We do not consider here $YBa_2Cu_3O_{7-\delta}$ (YBCO) and $Bi_2Sr_2CaCu_2O_{8+\delta}$ (Bi2212) with two CuO_2 layers in the unit cell where the bilayer splitting of the FS appears, so we calculate DOS for the electrons in the doped single CuO_2 layer.

The change of the FS topology at $x_{c1} = p_{opt}$ results in the logarithmic divergence of DOS (figure 2), while the emergence of the new electron-like pocket below $x_{c2} = p^*$ results in a step in the DOS (figure 3). The total DOS is a sum of the singular and regular contributions. We would like to stress that both logarithmic and step DOS singularities are in perfect agreement with the general properties of the van Hole singularities for the 2D electrons [43]. Contrary to the 3D systems, the thermodynamical potential for the 2D electrons has a singular contribution $\delta\Omega \sim (\varepsilon_F - \varepsilon_c)^2$ for the step singularity and $\delta\Omega \sim (\varepsilon_F - \varepsilon_c)^2 \ln|\varepsilon_F - \varepsilon_c|$ for the logarithmic singularity [44]. Thus QPT at $x_{c2} = p^*$ is of the second order, while at $x_{c1} = p_{opt}$ the singularity is stronger. It immediately follows that the Sommerfeld parameter γ in the electronic heat capacity $\gamma = C_e/T$ has also a singular step contribution at $x \leqslant p^*$, and

$$\delta\gamma \propto \ln(\varepsilon_F - \varepsilon_c) \propto \ln|x - x_{opt}| \qquad (2)$$

near $x_{c1} = p_{opt}$. Similar divergence in the specific heat

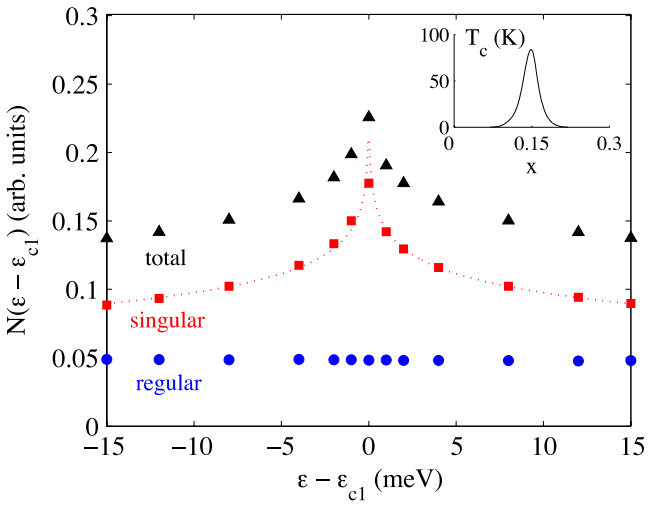

Figure 2. Regular, singular and total DOS $N(\varepsilon - \varepsilon_{c1})$ near the optimal doping, $\varepsilon_{c1} = \varepsilon_F(p_{opt})$, as calculated from the Green's function (1). The dotted line shows the logarithmic fitting. In the inset, the doping dependence of the superconducting critical temperature $T_c(x)$ is shown; the optimal doping is 0.151. Note that the energy $\varepsilon - \varepsilon_{c1}$ is the energy of holes.

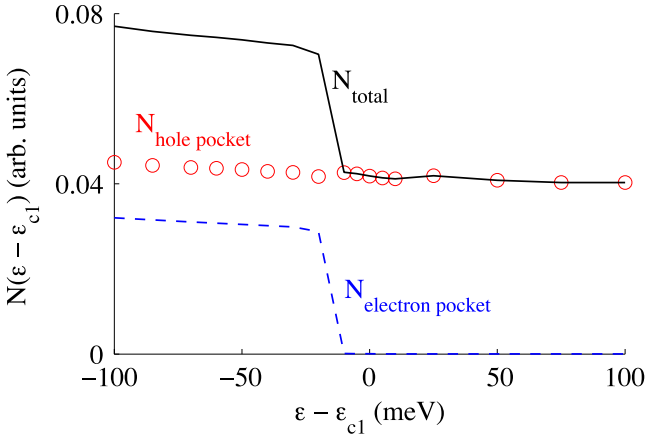

Figure 3. Regular (hole pocket), singular (electron pocket) and total DOS $N(\varepsilon - \varepsilon_{c1})$ near the pseudogap critical point $\varepsilon_{c2} = \varepsilon_F(p^*)$. Below $p^* = 0.24$ ($\varepsilon < \varepsilon_{c2}$) a singular step-like contribution to the total DOS appears. Note that the energy $\varepsilon - \varepsilon_{c1}$ is the energy of holes.

was found within the dynamical cluster approximation for the Hubbard model [45].

To check whether the coincidence of x_{c1} with p_{opt} and x_{c2} with p^* is occasional or not, we have calculated the superconducting critical temperature dependence $T_c(x)$ in the same model [46] and the kinetic energy as a function of doping. The $T_c(x)$ dependence is an inverse parabola with the maximum at x_{opt} (see inset in figure 2), which indeed equals x_{c1}. Note that it is not a coincidence since, like in the BCS theory, the maximum in $T_c(x)$ is determined by the maximum DOS, and at x_{c1} we have a logarithmic singularity. Kinetic energy, $E_{kin} = \sum_n t_{0n}^{11} K_{0n}$, reveals a remarkable kink at $x_{c2} = p^*$ (figure 4). Above p^*, $E_{kin}(p)/E_{kin}(p^*) \sim 1 + p$, which is expected for a conventional 2D metal with hole

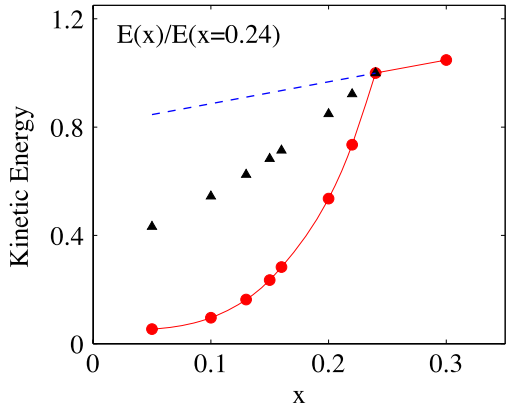

Figure 4. The doping dependence of the dimensionless kinetic energy $E_{kin}(p)/E_{kin}(p^*)$. The calculated dependence is shown by the filled (red) circles. Above p^* it obeys a conventional law and is proportional to $(1 + p)$. The extrapolation of this law to the region $p < p^*$ (blue dashed line) emphasizes the depletion of part of the kinetic energy in the pseudogap region. The calculation for the idealized triangular pseudogap model (3) is shown by the filled triangles.

concentration $n_h = 1 + p$ and $E_{kin} \sim \varepsilon_F \sim n_h$. The extrapolation of this law below p^* (shown in figure 4 by the blue dashed line) reveals that the actual E_{kin} is smaller. We associate this depletion of the kinetic energy with the pseudogap formation and try to fit it with a simple free electron gas with a triangular pseudogap DOS (Loram–Cooper model [1, 2]):

$$N(\varepsilon) = \begin{cases} g, & |\varepsilon - \varepsilon_F| > E_g \\ g\dfrac{|\varepsilon - \varepsilon_F|}{E_g}, & |\varepsilon - \varepsilon_F| < E_g. \end{cases} \quad (3)$$

Here $E_g = J(p^* - p)/p^*$ is a doping dependent pseudogap and J is the nearest neighbor exchange parameter. This fitting is shown by the filled triangles and it reflects some decrease of the kinetic energy due to the pseudogap but does not provide a quantitative agreement. Apparently, better fitting is given by the exponential law, $E_{kin}(p)/E_{kin}(p^*) = \exp[-4E_g(p)/J]$. This analysis confirms that the QPT at x_{c2} is indeed related to the pseudogap and the coincidence of x_{c2} and p^* is not occasional.

A singular contribution to the Hall coefficient near the optimal doping has been measured for $Bi_2Sr_{0.51}La_{0.49}CuO_{6+\delta}$ single crystals and for $La_{2-x}Sr_xCuO_4$ thin films under a strong magnetic field of 60 T [8]. According to our theory, these extra carriers are induced by the singular DOS. To continue discussion in terms of the critical points, not the critical energies, we note that near the critical point $\varepsilon_F(x) - \varepsilon_{c1} = k(x - x_{opt})$. In figure 5 we plot the calculated singular DOS $N_{sing}(z)$, $z = x - x_{opt}$, together with the singular contribution to the Hall coefficient, $n_{Hall}(1.5\ K) - n_{Hall}(100\ K)$ [8]. The optimal doping in the LSCO thin film $x_{opt} = 0.17$ is shifted from the bulk value $x_{opt} = 0.15$ in the Bi2201 which may be due to the strains in the films. The general agreement of the calculated singular DOS and Hall data provides further support for our analysis.

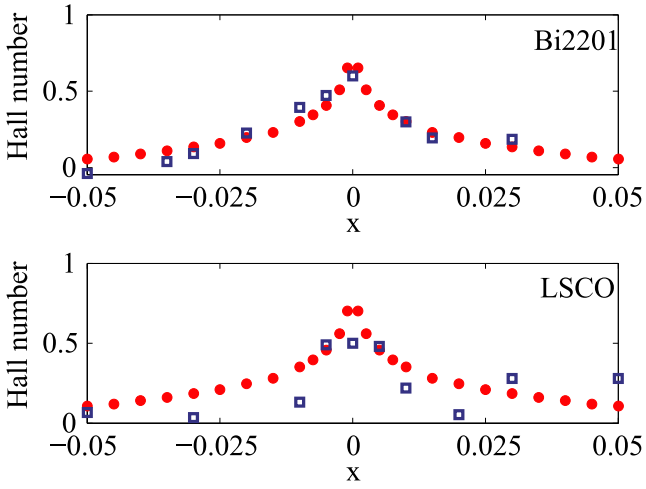

Figure 5. Comparison of experimental (blue squares) singular Hall coefficient [8] for $Bi_2Sr_{0.51}La_{0.49}CuO_{6+\delta}$ (a) and for $La_{2-x}Sr_xCuO_4$ (b) and our calculated (red filled circles) singular DOS, $N_{\rm sing}(\varepsilon_{\rm F}(x))$, near the optimal doping as follows from equation (2). Agreement with results on bulk single crystals (a) is better than with results on thin films (b).

4. Discussion

Now we are going to compare our results with the other relevant studies and discuss the retardation effects for the electronic self-energy. These effects determine Im $\Sigma(\mathbf{k}, \omega)$ and hence the quasiparticle spectral weight and line width. Our approach allows us to go beyond the static limit and to get the frequency dependent real and imaginary parts of the self-energy by the Mori-type projection technique; for the Hubbard model, calculations of such type have been done in [31]. The authors of [31] obtain very similar concentration dependence of the FS (see figure 6 in their paper) as we have. This agreement proves that Im $\Sigma(\mathbf{k}, \omega)$ is not so important for the shape of the FS. Nevertheless it is important for the spectral weight. In particular, the spectral weight of the inner pocket around (π, π) is small due to the finite quasiparticle lifetime. Thus the ARPES intensity for this pocket is small and that may be the reason why it has never been observed by ARPES.

The energy dependence of the electron self-energy is crucial and determines the Mott–Hubbard transition in the Hubbard model, as was convincingly demonstrated by the dynamical mean-field theory (DMFT) [47]. Cluster generalization of DMFT [48–51] is necessary to study electron correlations in a 2D CuO_2 layer where the nearest neighbor spin correlations require the momentum dependent self-energy. The cellular DMFT (CDMFT) method provides k dependent self-energy and results in the phase diagrams that have features similar to the ones experimentally observed in cuprates [52–56]. Recently, the exact diagonalization version of CDMFT (CDMFT + ED) was used to study the electronic structure of the doped Mott–Hubbard insulator [57, 58]. The sequence of the FS transformations with doping in [57, 58] is very similar to ours. At a small doping x, four-hole pockets expand with x until they touch the Brillouin zone boundary ($|k_x|$ or $|k_y|$ equal to π). Then at $x_{c1} = p_{\rm opt}$ they merge into two concentric FSs around (π, π). With further doping, the smaller surface disappears leaving a large hole-like FS which later transforms into a normal electron-like one through one more Lifshitz QPT. In spite of many differences in details (for example both poles and zeros of the Green's function are obtained in [57, 58]) the similarity of the FS transformations in our work and papers [57, 58] proves the validity of our approach at least at low temperatures. We believe that it is the simplest approach that allows us to obtain the FS transformation from the lightly doped Mott insulator up to the Fermi liquid. Nevertheless our static approximation cannot treat the quasiparticle spectral weight (see discussion of [31] above). It does not work in the Fermi liquid regime either. We start our perturbation theory with the small self-energy in the atomic limit and then the self-energy will be large in the band limit.

One more agreement between our work and the dynamical cluster approximation is the $T^2 \log T$ singularity in the thermodynamic potential at x_{c1} in [45] and our $z^2 \log z$ (see equation (2)) at the Lifshitz QPT. At zero temperature, z is given by the energy difference of the Fermi level and the critical energy, which is proportional to $(x - x_{c1})$. At finite temperature $z \propto T$.

5. Conclusion

We have shown that there are two critical points in the cuprate's doping dependence. The first one is related to the change of the FS connectivity and logarithmic divergences of DOS and of the electronic heat capacity parameter γ at the optimal doping $p_{\rm opt} = 0.151$. Also, we associate this QPT with the experimentally observed singular doping dependence of the Hall coefficient [8]. Moreover, the logarithmic enhancement of DOS leads to the maximum in the doping dependence of the superconducting critical temperature T_c at the same critical point $x = p_{\rm opt}$. This is in agreement with the previous calculations of T_c for the magnetic mechanism of $d_{x^2-y^2}$ pairing. The second QPT is associated with the collapse of the electron-like FS pocket at $p \to p^* = 0.246$ and results in the step singularities in DOS and in the Sommerfeld parameter γ. We have found the depletion of the hole's kinetic energy below p^* and ascribe it to the pseudogap formation at $p < p^*$. Thus the two energy scales in cuprates measured by T_c and T^* are both related to the QPTs and to the changes of the cuprate's electron structure with doping. The very existence of both logarithmic and step singularities in DOS are in perfect agreement with the general properties of the van Hole singularities for the 2D electron systems. But the concentrations of doping at which these singularities approach the Fermi level and start to govern the behavior of the system are determined by the strong electronic correlations and scattering on the associated short-range AFM order.

Note that our analysis is appropriate for cuprates that have one CuO_2 layer in the unit cell. The question arises as to whether the model parameters and corresponding critical concentrations are the same for e.g. LSCO and Bi2201. In the conventional single-electron tight-binding model with the rigid band the hopping parameters depend significantly on

doping. That is why the ratio t'/t extracted from ARPES is usually different for Bi2201 and LSCO. In general, the hopping parameters depend on the interatomic distance, which is almost the same in these two crystals. That is why we use the same parameters for all doping concentrations. The doping dependence of the band structure and its non-rigid behavior appear as an effect of strong electronic correlations.

Acknowledgments

We would like to thank S Sakai for useful discussions. The authors acknowledge support by the Russian Foundation for Basic Research (grant N 09-02-00127), by the Integration Program of SBRAS N40, the Presidium RAS Program 5.7, President of Russia (grant MK-1683.2010.2), FCP Scientific and Research-and-Educational Personnel of Innovative Russia for 2009-2013 (GK P891), and in part by the National Science Foundation under grant NSF PHY05-51164.

References

[1] Cooper J R and Loram J W 2000 *J. Physique* IV **10** Pr3-213
[2] Loram J W, Luo J, Cooper J R, Liang W Y and Tallon J L 2001 *J. Phys. Chem. Solids* **62** 59
[3] Tallon J L, Loram J W, Williams V M G, Cooper J R, Fisher I R, Johnson J D, Staines M P and Bernhard C 1999 *Phys. Status Solidi* b **215** 531
[4] Castellani C, Di Castro C and Grilli M 1997 *Z. Phys.* B **103** 137
[5] Daou R *et al* 2009 *Nat. Phys.* **5** 31
[6] Hüfner S, Hossain M A, Damascelli A and Sawatzky G 2008 *Rep. Prog. Phys.* **71** 062501
[7] Balakirev F F, Betts J B, Migliori A, Ono S, Ando Y and Boebinger G S 2003 *Nature* **424** 912
[8] Balakirev F F, Betts J B, Migliori A, Tsukada I, Ando Y and Boebinger G S 2009 *Phys. Rev. Lett.* **102** 017004
[9] Damacelli A, Hussein Z and Shen Z-X 2003 *Rev. Mod. Phys.* **75** 473
[10] Meng J *et al* 2009 *Nature* **462** 335
[11] Lifshitz I M 1960 *Zh. Eksp. Teor. Fiz.* **38** 1569
Lifshitz I M 1960 *Sov. Phys.-JETP* **11** 1130 (Engl. Transl.)
[12] Horsch P, Stephan W, von Szczepanski K J, Ziegler M and von der Linden W 1989 *Physica* C **162** 783
[13] von Szczepanski K J, Horsch P, Stephan W and Ziegler M 1990 *Phys. Rev.* B **41** 2017
[14] Preuss R, Hanke W and von der Linden W 1995 *Phys. Rev. Lett.* **75** 1344
[15] Elesin V F and Koshurnikov V A 1994 *JETP* **79** 961
[16] Shraiman B I and Siggia E D 1988 *Phys. Rev. Lett.* **61** 467
[17] Trugman S A 1990 *Phys. Rev. Lett.* **65** 500
[18] Barabanov A F, Kuzian R O and Maksimov L A 1991 *J. Phys.: Condens. Matter* **3** 91129
[19] Chen W Q, Yang K Y, Rice T M and Zhang F C 2008 *Europhys. Lett.* **82** 17004
[20] Kane C L, Lee P A and Read N 1989 *Phys. Rev.* B **39** 6880
[21] Martinez G and Horsch P 1991 *Phys. Rev.* B **44** 317
[22] Thurston T R *et al* 1989 *Phys. Rev.* B **40** 4585
[23] Kampf A P 1994 *Phys. Rep.* **249** 222
[24] Schmalian J, Pines D and Stojkovic B 1999 *Phys. Rev.* B **60** 667
[25] Kuchinskii E Z and Sadovskii M V 1999 *JETP* **88** 968
[26] Anderson P W 1987 *Science* **235** 1196
[27] Baskaran G, Zhou Z and Anderson P W 1987 *Solid State Commun.* **63** 973
[28] Pathak S, Shenoy V B, Randeria M and Trivedi N 2009 *Phys. Rev. Lett.* **102** 027002
[29] Senthil T 2008 *Phys. Rev.* B **78** 035103
[30] Korshunov M M, Gavrichkov V A, Ovchinnikov S G, Nekrasov I A, Pchelkina Z V and Anisimov V I 2005 *Phys. Rev.* B **72** 165104
[31] Plakida N M and Oudovenko V S 2007 *JETP* **104** 230
[32] Harrison N, McDonald R D and Singleton J 2007 *Phys. Rev. Lett.* **99** 206406
[33] Korshunov M M and Ovchinnikov S G 2007 *Eur. Phys. J.* B **57** 271
[34] Barabanov A F, Hayn R, Kovalev A A, Urazaev O V and Belmuk A M 2001 *JETP* **92** 677
[35] Prelovšek P 1997 *Z. Phys.* B **103** 363
[36] Plakida N M and Oudovenko V S 1999 *Phys. Rev.* B **59** 11949
[37] Liu Z and Manousakis E 1992 *Phys. Rev.* B **45** 2425
[38] Shimahara H and Takada S 1991 *J. Phys. Soc. Japan* **60** 2394
[39] Val'kov V and Dzebisashvili D M 2005 *JETP* **100** 608
[40] Hozoi L, Laad M S and Fulde P 2008 *Phys. Rev.* B **78** 165107
[41] Chakravarty S and Kee H-Y 2008 *Proc. Natl Acad. Sci. USA* **105** 8835
[42] Sachdev S, Chubukov A V and Sokol A 1995 *Phys. Rev.* B **51** 14874
[43] Ziman J M 1964 *Principles of the Theory of Solids* (Cambridge: Cambridge University Press)
[44] Nedoresov S S 1966 *Zh. Eksp. Teor. Fiz.* **51** 868
Nedoresov S S 1967 *Sov. Phys.-JETP* **24** 578 (Engl. Transl.)
[45] Mikelsons K, Khatami E, Galanakis D, Macridin A, Moreno J and Jarrell M 2009 *Phys. Rev.* B **80** 140505(R)
[46] Shneyder E I and Ovchinnikov S G 2006 *JETP Lett.* **83** 394
[47] Georges A, Kotliar G, Krauth W and Rozenberg M 1996 *Rev. Mod. Phys.* **68** 13
[48] Hettler M H, Tahvildar A N-Z, Jarrell M, Pruschke T and Krishnamurthy H R 1998 *Phys. Rev.* B **58** R7475
[49] Kotliar G, Savrasov S Y, Pálsson G and Biroli G 2001 *Phys. Rev. Lett.* **87** 186401
[50] Potthoff M 2003 *Eur. Phys. J.* B **32** 429
[51] Maier T, Jarrell M, Pruschke T and Hettler M H 2005 *Rev. Mod. Phys.* **77** 1027
[52] Sénéchal D, Lavertu P-L, Marois M-A and Tremblay A-M S 2005 *Phys. Rev. Lett.* **94** 156404
[53] Kancharla S S, Kyung B, Sénéchal D, Civelli M, Capone M, Kotliar G and Tremblay A-M S 2008 *Phys. Rev.* B **77** 184516
[54] Haule K and Kotliar G 2007 *Phys. Rev.* B **76** 104509
[55] Macridin A, Jarrell M, Maier T and Sawatzky G A 2005 *Phys. Rev.* B **71** 134527
[56] Kyung B, Sénéchal D and Tremblay A-M S 2009 *Phys. Rev.* B **80** 205109
[57] Sakai S, Motome Y and Imada M 2009 *Phys. Rev. Lett.* **102** 056404
[58] Sakai S, Motome Y and Imada M 2010 *Phys. Rev.* B **82** 134505